

Review

Dye Decoloring Peroxidase Structure, Catalytic Properties and Applications: Current Advancement and Futurity

Lingxia Xu [†], Jianzhong Sun [†] , Majjid A. Qaria [†], Lu Gao and Daochen Zhu ^{*} 

Biofuels Institute, School of the Environment and Safety Engineering, Jiangsu University, 301# Xuefu Road, Zhenjiang 212013, China; xulingxia@stmail.ujs.edu.cn (L.X.); jzsun1002@ujs.edu.cn (J.S.); majidqaria@gmail.com (M.A.Q.); lgao@ujs.edu.cn (L.G.)

* Correspondence: dczhucn@ujs.edu.cn

[†] These authors have contributed equally to this work.

Abstract: Dye decoloring peroxidases (DyPs) were named after their high efficiency to decolorize and degrade a wide range of dyes. DyPs are a type of heme peroxidase and are quite different from known heme peroxidases in terms of amino acid sequences, protein structure, catalytic residues, and physical and chemical properties. DyPs oxidize polycyclic dyes and phenolic compounds. Thus they find high application potentials in dealing with environmental problems. The structure and catalytic characteristics of DyPs of different families from the amino acid sequence, protein structure, and enzymatic properties, and analyzes the high-efficiency degradation ability of some DyPs in dye and lignin degradation, which vary greatly among DyPs classes. In addition, application prospects of DyPs in biomedicine and other fields are also discussed briefly. At the same time, the research strategy based on genetic engineering and synthetic biology in improving the stability and catalytic activity of DyPs are summarized along with the important industrial applications of DyPs and associated challenges. Moreover, according to the current research findings, bringing DyPs to the industrial level may require improving the catalytic efficiency of DyP, increasing production, and enhancing alkali resistance and toxicity.

Keywords: dye decoloring peroxidase; polycyclic dyes; phenolic compounds; environmental



Citation: Xu, L.; Sun, J.; Qaria, M.A.; Gao, L.; Zhu, D. Dye Decoloring Peroxidase Structure, Catalytic Properties and Applications: Current Advancement and Futurity. *Catalysts* **2021**, *11*, 955. <https://doi.org/10.3390/catal11080955>

Academic Editors: Yung-Chuan Liu, Si-Yu Li and Nien-Jen Hu

Received: 21 July 2021

Accepted: 9 August 2021

Published: 10 August 2021

Publisher's Note: MDPI stays neutral with regard to jurisdictional claims in published maps and institutional affiliations.



Copyright: © 2021 by the authors. Licensee MDPI, Basel, Switzerland. This article is an open access article distributed under the terms and conditions of the Creative Commons Attribution (CC BY) license (<https://creativecommons.org/licenses/by/4.0/>).

1. Introduction

The dye decoloring peroxidases ((DyP, EC 1.11.1.19) the systematic name is reactive-blue-5: hydrogen-peroxide oxidoreductase) belongs to the heme peroxidases family [1]. In 1999, for the first time, a DyP was identified and purified from the basidiomycete *Bjerkandera adusta*. Since then, over the past 20 years, research on DyPs has grown exponentially [2]. DyPs are bifunctional enzymes with both oxidative and hydrolytic activities. It can degrade some tenacious substrates, including dyes, β -carotene, aromatic compounds, and sulfides. Fascinatingly, they prefer anthraquinone dyes as a substrate and have a high enzymatic activity for various organic compounds [3]. However, these are due to DyPs' unique sequence and protein nature that differs from other known peroxidases [4]. Therefore, it has great application prospects in papermaking, coatings, environmental protection, bioenergy industries, etc.

In recent years, researchers focused on microbial DyPs and intensely observed their degradative supremacy, such as the degradation of dyes and lignin. Previous studies have clearly defined and explained the enzymatic structure and properties of DyPs, but its catalytic pathways for the degradation of dyes and lignin are still unclear. Although, DyPs have tremendous industrial and environmental applications. Unfortunately, several obstacles have hindered its industrial application, such as low industrial enzyme activity, foreign enzyme pollution, a complicated purification process, long growth cycle, and high cost. However, recently there have been several attempts to overcome these shortcomings and in the advancement in technologies and understanding of the catalytic pathways.

This review article comprehensively focuses on discussing the structure of DyPs and its tremendous applications. Moreover, we discuss the current uses and the obstacles that hinder the applications of DyPs in industry and different fields.

2. Composition and Structural Characteristics of DyPs

2.1. Sources and Classification of DyPs

Kim et al. (1999) discovered the first type of DyPs from fungi and named it for its ability to degrade various types of dyes. They characterized the first dye decolorizing protein in the fungus *Thanatephorus cucumeris* Dec 1 and isolated the first enzyme of the DyP family (BAD DyP) from the fungus [5]. Subsequently, various DyPs were isolated and characterized from different bacterial strains of DyP (Supplementary Table S1).

Peroxidase is an essential type of oxidoreductase, which contains heme protein, and an iron porphyrin IX as a prosthetic group exists in the active site. It is customary to divide heme peroxidases into two superfamilies: animal and plant peroxidase superfamilies. According to the homology of the primary structure, plant peroxidases are divided into categories I, II, and III, including fungal peroxidase (category II) and bacterial peroxidase (category I). Category I peroxidases have pigment C peroxidase, ascorbate peroxidase, and bacterial peroxidase [6].

Category II peroxidases are mainly peroxidases secreted by fungi, such as lignin peroxidase (LiP; EC 1.11.1.14), manganese peroxidase (MnP; EC 1.11.1.13), horseradish Peroxidase (HRP; EC1.11.1.7), and versatile peroxidase (VP; EC1.11.1.16) [7]. Enzymes of this category are extracellular and heme with different molecular characteristics such as the sequence of amino acids, protein 3D structure, catalytic activity, and environmental conditions. Some peroxidases secreted by plants, such as horseradish peroxidase and barley grain peroxidase, belong to the category III peroxidase [8]. The DyP forms a sandwich-shaped β sheet between the α helices. Traditional peroxidases are mainly composed of α helices and do not contain β sheets [9]. Studies have found that the DyPs enzyme has a high redox potential and can be used at pH 2–3. Anthraquinone dyes have high activity, while the other peroxidases do not have such characteristics [10]. Moreover, DyPs lacks plant peroxidase's typical amino acid sequence (R-X-X-F/W-H), R represents arginine, and H represents distal histidine. Due to these differences between DyPs and other peroxidases, the DyPs enzyme should be a new type of heme peroxidase, different to other peroxidases [3]. According to the difference of origin, PeroxiBase classification database DyP-type peroxidases superfamily divided into four Classes A to D (<http://peroxibase.toulouse.inra.fr>, accessed on 4 July 2021). Different DyPs enzymes of A, B, C, and D show very similar protein tertiary structures (Z score > 20), and amino acid sequences of different types of DyPs are quite different. For example, the amino acid homology between Class D and Classes A, B, and C are 7%, 7%, and 16%, respectively [4]. Using the MATRAS tool to obtain the sequence alignment based on the protein tertiary structure of DyP, a new classification scheme for the DyPs family was proposed. This classification contains three classes (Class I, Class P, and Class V), where Class C and Class D were classified into Class V, while Class A and Class B are classified into Class I and Class P [4]. This kind of tertiary structure analysis is adequate for further analysis because they reveal the fundamental structural similarity between different DyP-type peroxidases. Currently, scientists are more inclined to use the PeroxiBase classification procedures to classify DyPs. However, there are only two enzymes in the Class C family whose structure has been elucidated [11,12].

2.2. Characteristics of DyPs

There are 237 enzymes in the DyPs family entered in the RedoxiBase database and DyP Class D accounts for more than 1/2, reaching 138. The first DyP-type enzymes discovered belong to the D-type DyPs (Figure 1). The D-type DyPs discovered are all produced by fungi, such as IIDyP produced by *Irpex lacteus* [13], rPsaDyP produced by *Pleurotus sapidus* [14], and AauDyP2 produced by *Auricularia auricula-judae* [15]. D-type

DyP, as an extracellular enzyme, can be separated and purified from the microbial culture broth. Interestingly, these microorganisms often play a role in the degradation of lignin.

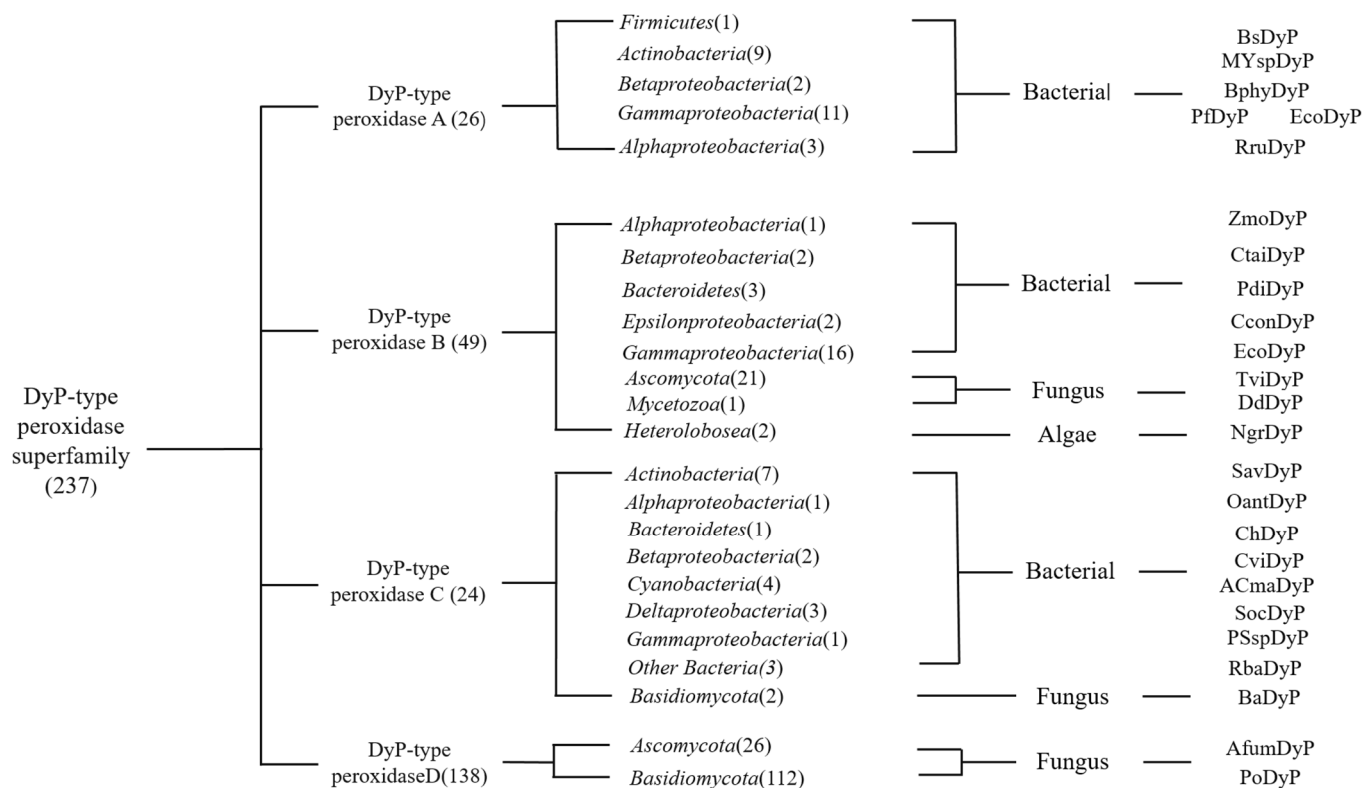


Figure 1. Phylogenetic graph details the DyPs classes in the database and the corresponding producing microorganisms.

In contrast, Class A DyP was mainly isolated from bacteria. In Class B and C DyP, the primary source is still bacteria and lower eukaryotes produce a small part. It is worth noting that DyP from algae is found in Class B DyP. Among the microbes, the production cost of DyP from algae is lower than that of microbes when achieving higher yields. The length of the encoding amino acid sequence, encoding the D-type DyP, is longer, followed by the C, A, and B classes. Moreover, D-type DyP expresses a higher oxidation capacity in the catalytic efficiency of lignin model compounds and dyes, and the catalytic efficiency of AauDyP2 and Ildyp to Reactive Blue 5 and Reactive Black 5, which can reach 5.6×10^6 and 1.7×10^7 in (K_{cat}/K_m) [13,15]. In addition, PsaPax also expresses high activity in olefin degradation [16]. Class C DyPs have various enzyme activities, such as DyP2 produced by actinobacteria *Amycolatopsis sp.* 75iv2. The electron transfer of hydrogen peroxide in the DyP2 catalytic process depends on the participation of Mn^{2+} , and Mn^{2+} is regulated by the enzyme [11]. In the crystal structure of DyP2, it was observed that Mn^{2+} is combined and Mn^{2+} can greatly improve the catalytic efficiency.

On the other hand, Class B DyPs' main characteristics are those specific protein-encoding genes and genes encoding capsular proteins are in operons form and form microcapsule structures that can protect DyPs [17]. In addition, some B-type DyPs, such as YfeX and YcdB, have the function of dechelating enzymes, which can extract an iron atom from heme without degrading the tetrapyrrole ring. The special features of Class A proteins are that some Class A proteins have two arginine ectopic (Tat) signal sequences at the N-terminus. It is confirmed that Class A enzymes rely on the TaT signal sequence to act outside the cytoplasm or the cell [18].

2.3. Structural Characteristics of DyP

Among the DyPs whose structures have been identified, including A, B, C, and D DyPs, it has been shown that it forms crystals in vitro with protoporphyrin (PPIX) at the heme-binding pocket except for EfeB [19]. DyPIn characterizes all DyPs and the binding pocket with an unclear function, and heme binds in the larger C-terminal region of the protein. In the wild-type DyP structure containing heme, the heme is coordinated by solvent molecules on the distal side, the coordination of type A DyPs occurs in the intermembrane zone, and the coordination of type C and D DyPs occurs at the C-terminal heme combination zone [20]. By observing the protein secondary structure of DyP, it was found that the heme propyl group was located in the centre of the molecule, and a large number of α and β helix layers were folded. It is conceivable that the tertiary structure of DYP is mainly composed of dimeric or polymeric α -helix and β -helix. From the perspective of the tertiary structure of DyPs, the new classification method proposed by Yoshida and Sugano will significantly promote the study [4]. For example, according to the common structural characteristics of Class C and Class D in the same structural region, Class C DyP and Class D DyP can be classified as Class V. The important amino acid residues of Class P (Class B) DyPs are contained in the structural backbone. In contrast, the protein structures of Class A and Class V (Class C and Class D) have some extra regions based on Class P. This seems to explain, from another aspect, why Class C and Class D DyP can express higher catalytic efficiency because the function of enzymes often depends on its internal protein structure skeleton. Class C and Class D are larger than Class A and Class B from the structure size.

In addition, the binding residues of heme include conserved residues in DyPs and other residues in specific categories. In all DyPs enzymes, the proximal axial ligand of the heme iron structure is His, and it forms a hydrogen bond with the carboxylate of the acidic residue. There are also three residues at the distal end of heme iron: Asp, Arg, and Phe. These residues are similar in position to each other, while Arg is the closest to heme iron (NH1 to Fe—4.3 Å) and is compatible with propionic acid [21]. In addition, the polar residue (Asn246 in DypB) in the B-type DyPs hemoglobin pocket interacts with the iron-coordinated solvent. Although this residue is not conserved in other types of DyP, it corresponds to Ser331 in DyP2 and Gly348 in DyPdec1, and its function seems to be related to the distance between heme iron and the coordination solvent [22,23]. An interesting example is a novel cytoplasmic DyPA from *Dictyostelium discoideum*, which has the capability to oxidize anthraquinone dyes and lignin model compounds. Unlike related enzymes, an aspartate residue replaces the first glycine of the conserved GXXDG motif in *Dictyostelium* DyPA. The active site of *Dictyostelium* DyPA has a hexa-coordinated heme iron with a histidine residue at the proximal axial position and either activated oxygen or a CN^- molecule at the distal axial position [24].

2.4. The Physical and Chemical Properties of DyPs

Among all DyPs identified, except for a small number of bacteria that produce DyPs whose molecular weight is less than 40 kDa, the molecular weights of other enzymes are concentrated in 50–60 kDa, containing heme protein. There is an iron porphyrin IX at the active site [25]. DyPs mainly exist in the form of monomers, dimers, tetramers, and hexamers. Numerous studies have shown that DyP will maintain a high activity under acidic conditions, using 2,2-diaza-bis(3-ethyl-benzothiazole-6-sulfonic acid) diammonium salt (ABTS) as a substrate. In the enzyme activity test, the optimum pH of DyP is generally between 4.0 and 5.0. When SBP (soybean peroxidase) and CiP (generic peroxidases of *Coprinopsis cinerea*) are used as substrates, the optimum enzyme activity is 5.5 and 6.8 [15], respectively. For example, when BsDyP, PfDyP, and PpDyP are based on ABTS, 2,6-dimethoxyphenol, the optimal pH of DyP is mainly distributed between pH levels 2.0–4.0, 4.0–7.2, and 3.0–5.5, while the optimum pH varies [26]. In the practical application of DyPs, the optimal pH must ensure the high activity of DyP and consider the stability of DyP. Lier et al. have tested the pH catalytic effect on various DyPs and observed that although AauDyP1 has a high pH of 3.0 in an acidic environment, the activity is strong. At the same

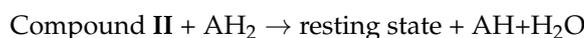
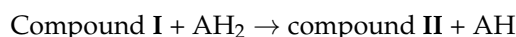
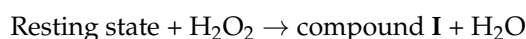
time, the stability of DyP is poor. Another study has observed that DyP has a stronger stability correlated with a lower activity when the pH value increases.

In addition, the temperature has a greater influence on enzyme activity. The optimal temperature of DyP is mainly concentrated at 40–60 °C [20]. Previously, the TfuDyP reaction rate was the highest at 45–60 °C at pH 5.5 utilizing DCP as a substrate, and the reaction rate decreases linearly as the temperature rises [27].

However, to use DyPs in industrial applications, it is crucial to coordinate the tolerance of pH and temperature and broaden the temperature and pH activity range. Various metal ions such as Ca^{2+} , Mg^{2+} , Zn^{2+} , Fe^{2+} , Mn^{2+} , Co^{2+} , Hg^{2+} , Pb^{2+} and Pd^{2+} can also have an important impact on DyP activity. Previously, the effect of various ions on DyP B was investigated and it was found that Ca^{2+} , Zn^{2+} , and Mn^{2+} all make extracellular laccase activity and an increased effect of Zn^{2+} is the most significant [28]. Some metal ions such as Fe^{2+} and Hg^{2+} also have a strong inhibitory effect on DyP. Inhibition of Fe^{2+} may destroy the hydrogen peroxide transfer mechanism of DyP and make DyP itself active, while other ions may be in the process of reaction. These metal ions occupy the active centre of the DyP, change the structure of the DyP, and block the substrate's binding with DyP, thereby inhibiting the enzyme activity. At the same time, Loncar also tested the effect of several inhibitors of aminotriazole, EDTA, imidazole, DTT, Cys, and sodium azide on enzyme activity. Under an inhibitory concentration of 0.5 mmol/L for DTT, Cys, and azide, the inhibitory effect of sodium sulfide on DyP was distinct, completely inhibiting the activity of DyP [20]. The inhibitory activity of aminotriazole is the lowest. DyP can still maintain around 60% of the activity. Still, the final complete inhibitory concentration of aminotriazole, EDTA, and imidazole has not been tested, and the tolerance of DyPs from different sources to inhibitors varies greatly and the tolerance of DyPs may also change accordingly after recombinant expression [27].

2.5. Catalytic Characteristics and Mechanism

Under normal conditions, DyP-type peroxidase shows a typical peroxidase activity, and the catalytic mechanism of DyP is the same as other heme peroxidases. As shown in Figure 2A, H_2O_2 first reacts with enzymes to oxidize heme (Fe^{3+} por) during the peroxidation cycle to generate compound I (porphyrin cationic radical intermediate). The substrate first reduces redox compound I to compound II and then continues to pass through a single electron reducing compound II and forms an enzyme in a resting state [23].



With the deepening of research, compound I and compound II can exist in a separate state during the redox process of DyP. For example, the intermediate of compound II can be found in the research of DyPA, EfeB and BsDyP, but compound I was not detected; these enzymes are all Class A DyPs [19,25,29]. Interestingly, under the condition of pH 7.8, compound II, H_2O_2 and hydroquinone were observed at the same time for TcDyP. Still, under the condition of pH 3.0, compound II was not observed, which are precisely the wild-type TcDyP Optimal conditions for the catalytic reaction [30]. The presence of compound II was not detected under acidic conditions for Class B DyPs and Class D DyPs, which means that pH may be used as a reference condition for future research directions. Based on the reaction conditions where only the chemical compound I exists, a new two-electron catalytic mechanism is proposed, and the compound I directly undergoes two-electron reduction to become a resting state [30]. As shown in Figure 2B, after undergoing the deprotonation of hydrogen peroxide, the amino acid acts as a source of alkalinity. Finally, it reacts to produce the Fe (III)-OOH, which is compound 0. However, the reaction of compound 0

was so fast that it can hardly be detected, and the O-O bond breaks to form compound I. B-type DyP and the D-type DyP can be directly converted from compound I to the resting state under the condition that the presence of compound II cannot be detected, while the A-type DyP can be directly combined by compound I when the presence of compound I cannot be detected. Compound II directly changes to the resting state. However, the catalytic mechanism of Class C DyP is still unclear. According to the parental properties of homologous sequences, it is always classified as Class D DyP.

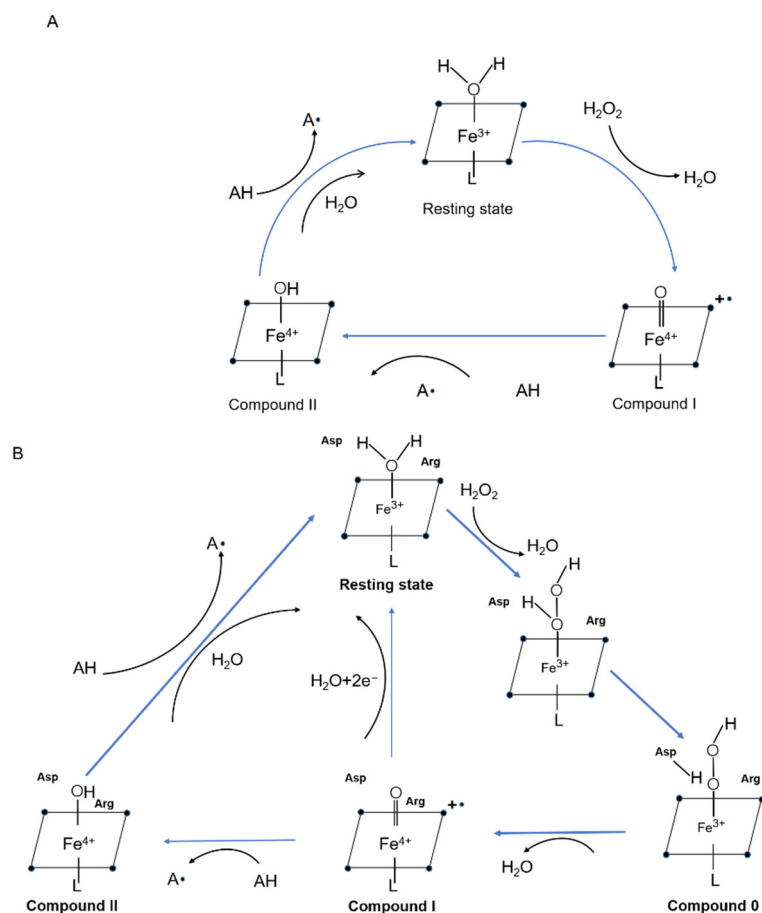


Figure 2. The typical catalytic cycle of heme peroxidases. The square represents the heme plane in the enzyme. AH stands for the substrate. (A) Conventional peroxidase catalyzed reaction mechanism. (B) catalytic mechanism of different DyPs. The activity of DyP-type peroxidase depends on the amino acid residues in the center of the enzyme that has the ability to catalyze aspartic acid and arginine.

DyP-type peroxidases contain the so-called GXXDG motif in their primary sequence, part of the heme-binding region. This motif is essential for peroxidases activity because the substitution of Ala or Asp for the conserved aspartic acid will inactivate the enzyme, and heme-binding will not be affected. Suggo et al. observed that in DyP produced by *Bjerkandera adusta*, ASN replaced D171, resulting in a 3000-fold reduction in its catalytic activity [10]. Similarly, the substitution of D153 by Ala in the DypB produced by *R. jostii* reduced the formation rate of compound I and the substitution of Arg-244 by Leu resulted in the loss of DypB activity [31]. In addition, DyP produced by *Thermobifida fusca* can sulphate lignin with a strong oxidation ability. Still, when Ala replaces D203, its catalytic constant was reduced 30-fold, while Gln replaces R315, the enzyme activity was completely lost [27]. This leads to a sharp decline in peroxidase activity, highlighting the critical importance of aspartic acid in GXXDG. Brissos et al. used continuous error-prone PCR technology to design DyP peroxidase in *Pseudomonas putida* MET94 to oxidize phenolic compounds. The designed three mutation points (E188 K, A142 V, H125Y) were far

away from the active site, but the catalytic efficiency of 2,6-dimethoxyphenol is increased 100 times [32]. These findings support that the DyP-type peroxidase relies on amino acid residues with the ability to catalyze aspartic acid and arginine.

2.6. Unrepresentative Characteristics, a Multifunctional Enzyme

The unique structure of DyP-type enzymes in their family makes these enzymes show multifunctional properties. For example, YfeX and YcdB showed the efficiency of removing ferrochelatase and strangely reacted with the iron in the blood-red cell without coordination with the hemoglobin skeleton, which is entirely different from the conventional DyPs [33,34]. Interestingly, it is observed that whether compound I or compound II is involved in the reaction process, the catalytic reaction of DyP is inseparable from the participation of H₂O₂ in principle. However, MscDyp from *Malassezia skrjabini* showed the absence of hydrogen peroxide. Similar to psapox, DyP was the first DyP with an olefin oxidation ability [16]. In anthraquinone dye degradation, it was demonstrated that BadDyP could cleave reaction Blue 5 and get phthalic acid. It is worth thinking that these DyPs with multifunctional properties seem to have a more practical application value, and some enzymes have been industrialized. Compared with other DyPs, it shows better talent in the industrial application of DyPs. Around the research and exploration of multifunctional DyPs, it may become a research hotspot in the practical application of DyPs in the future.

3. Application of Dye Decoloring Enzyme

The unique structure and catalytic characteristics of DyP proved that it should have broader uses in practical applications. Currently, the studies on the application of DyP is relatively less, and there are few successful industrial applications of DyP (Table 1).

Table 1. DyP biological characteristics and application prospects.

DyP Type	Summary of Findings on DyP	Biotechnological Potential	Ref
PfuDyP	Has a toxic effect on cells	Higher prospects in the medical field	[35]
SviDyP	<i>E. coli</i> heterologous expression	Improved alkali resistance of DyP to lignin environment	[36]
BsDyP	Degradation of lignin derivatives	Production of Veratrum aldehyde and other substances	[37]
TcDyP	Degradation of lignin derivatives	Strong activity on a variety of lignin substrates	[25]
TfuDyP	Degradation of lignin derivatives	Oxidation of phenolic substances couples the substrate to produce dimers	[27]
rPsaDyP	Heterologous expression strains for degradation	ABTS oxidation and pigment bleaching	[14]
CcP	Artificial introduction of amino acid residues	Man-made structure speeds up the reaction rate	[38]
BsDyP	Synergistic with laccase Cue0	Efficiently degrade melanin	[39]
PpDyP	Directed evolution technology transforms mutant DyP	High-sensitivity biosensor	[32]
PsaPOX	DyP can degrade a variety of olefins	The pyrolysis product will produce anisaldehyde	[16]

3.1. Lignin Degradation

As one of the most abundant energy materials on the earth, lignin is considered the material with the most potential to replace the fossil energy. Lignin is a highly crosslinked aromatic heterocyclic compound, polymerized by 4-dihydroxyphenylalanine through various ether bonds and C-C bonds, which is extremely difficult to biodegrade [40]. The microorganisms currently discovered that could degrade lignin are mainly rot fungi, *Pseudomonas*, *Sphingomonas*, *Rhodococcus jostii* RHA1, *phingobium* sp. SYK-6, *Bacillus ligniniphilus* L1 and *Streptomyces coelicolor*, etc. [41,42]. The ability of bacteria and fungi to degrade lignin is mainly dependent on four major heme peroxidases, including lignin peroxidase

(LIP), manganese peroxidase (MnP), multifunctional peroxidase (VP), and laccase (Lac), these enzymes can directly attack the lignin, cellulose, and hemicellulose of plant cells to cause it to be lysed [43]. Some properties of DyPs indicate that they may participate in the degradation of lignin. For example, when AauDyP oxidizes large-volume substrates, the surface will form exposed active free radicals similar to those produced when Lip and Vip catalyze tryptophan [15]. Various DyPs produced by fungi and bacteria have been proven to oxidize dye substrates with large molecular weights [44]. Most fungal DyP may be involved in catalyzing tryptophan residues. In addition, white-rot fungi DyP coding genes showed high efficiency in decomposing lignin; the coding genes are more abundant than brown rot fungi with a low lignin decomposition efficiency [45].

It has been shown that when lactic acid was added to produce DyP, the hydrolysis efficiency of wheat straw by White Harrowtooth fungus was improved by adding, which proved that DyPs could degrade lignin [20]. DyP can degrade and transform some mono, di, and poly lignin substrates. When studying BsDyP produced by *B. subtilis* KCTC2023, the BsDyP showed a higher enzymatic activity to ABST. Adding H_2O_2 under the reaction conditions of pH 3.0 and 50 °C, BsDyP cleaved the $C_\alpha-C_\beta$ bond and the produced β -O-4 bond dimeric lignin model compound isopropylglycerol- β -guaifenesin (VGE) is converted into veratraldehyde, the conversion efficiency reaches 53.5% within two h, and veratraldehyde is widely used as a flavor in the food industry (Figure 3C) [37]. In the process of lignin degradation, the peroxidase which can directly degrade lignin must have the ability to oxidize non-phenolic alkoxy aromatic groups. At present, the only exception is that some decomposing lignin peroxidases can oxidize some fungal metabolites, such as resveratrol, to produce aryl cation radical intermediates and then replace peroxidases to produce new oxidants to oxidize lignin. However, the reaction process still needs the participation of highly oxidizing peroxidases [46].

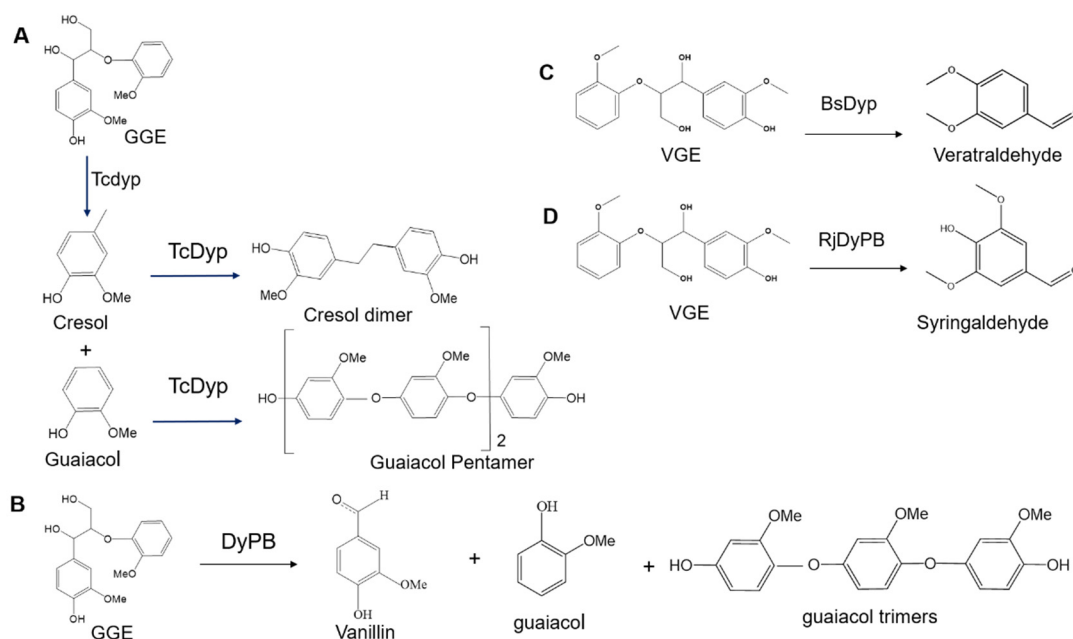


Figure 3. Lignin degradation reactions were listed. (A) tcDyP Degradation of GGE by TcDyP to produce a polymer. (B) Degradation of GGE to vanillin by DyPB. (C) Degradation of VGE to Veratraldehyde by BsDyP. (D) Degradation of VGE to Syringaldehyde by TfuDyP.

Compared with laccase, DyP has the ability to simultaneously oxidize phenolic and non-phenolic substrates. For instance, when H_2O_2 was added to acetic acid buffer solution at pH 6.0 to TfuDyP on lignin substrate and mixed with guaiacylglycerol- β - the dimerization of guaiacyl ether (GGE) occurred. The results of HPLC and GC-MS showed that TfuDyP did not cleave the ether bond of the substrate but oxidized the phenolic part

to couple the substrate with GGE. It was speculated that this was a dimer containing a biphenyl structure [27]. Another study on the degradation of the lignin model dimer GGE by bacterial DyPs found that TfuDyP did not cleave the ether bond of GGE but oxidized the phenol part, mainly producing a lignin dimer and trimer. In the oxidation of lignin phenols, the products usually exist in the form of polymers. Some compounds produced by the treatment of lignin model substrate with TcDyP are identified as a guaiacol pentamer and a cresol dimer (Figure 3A). In the oxidation of non-phenol, DyP may also play the decarboxylation function. The A-type TcDyP of *hermomonospora curvata* has a broad substrate range, making the non-phenol lignin substrate 4-methoxymandelic acid decarboxylate, and produces anisaldehyde as the final product. Still, it has no catalytic activity for resveratrol with a non-phenol structure. Decarboxylation usually plays a vital role in the degradation of lignin substrate [25,29].

In addition, dypase has a high stability at a low pH, and the optimal pH is different for the oxidation of phenolic and non-phenolic substances. Although it has been reported that DyPs activity can still maintain 50–90% after exposure to pH 2.5 for four hours, all the five reported DyPs can oxidize phenolic substrate 2,6-dimethoxyphenol; when the pH is below 3.0, the effect is optimum [15]. Dolores found that fungi had unique advantages in the oxidation of the non-phenol dimer model and showed a higher electric potential EO when comparing the decolorization peroxidase of bacteria and fungi dyes. When bacterial DyPs are more likely to attack phenol dimers, this means that bacteria are more likely to convert the decomposition products of natural lignin and are more suitable to some high phenol industrial lignin (pulp industry and biological transformation of ethanol industry).

On the other hand, it has been shown that DyP plays an active role in the treatment of lignin, and the transformed products can be used in medicine, food, energy, and other aspects, which can transform lignin into high-value products. In addition to resveratrol and Anisic Acid mentioned above, guaiacol, guaiacol trimer, and vanillin can be obtained from GGE treated with DyPB (Figure 3B). Based on a N246a mutant of *R. jostii* RHA1, DyPB was purified by Singh β -Aromatic ether compounds are mainly nitrated lignin, sulfate lignin, GGE, and other lignin related substrates. The degradation products are mainly syringaldehyde by HPLC and GC-MS (Figure 3D). Syringaldehyde is now widely used in medicine, high-grade spices, and pesticide chemistry industries.

Meanwhile, the conversion efficiency of syringaldehyde increased by 5.4–23 times when Mn^{2+} was added [29]. The addition of Mn^{2+} can improve the catalytic efficiency of DyPs to lignin substrate. The above studies revealed the biotechnology potential of DyPs in lignin degradation and proved that lignin could be used as a suitable substrate for lignin degradation. Although it is established that DyPs can degrade lignin, there are few reports on the mechanism and molecular mechanism of lignin degradation. With the further study of DyP, DyP is suitable for more lignin and its derivative substrates. At the same time, the progress of genetic and metabolic engineering technology also accelerates the universal applicability of DyPs to lignin. It overcomes the limitations of physical and chemical factors in its application. The engineering of *Pseudomonas fluorescens* DyP enhanced the enzyme catalysis of sulfate lignin degradation [47]. The lignin degradation activity of DyPs indicates its prospect in biorefinery because delignification was the main stage of lignocellulosic biomass conversion to ethanol [48]. A large amount of lignin will be produced in the pulp and paper industry as a by-product of the sulfate process; about 60–100 kilotons of sulfate lignin will be produced in a year [49]. With the world advocating the green economy of encouraging the production of biofuels from renewable resources, the accumulation of lignin in the environment is inevitable. Therefore, the emerging potential of DyP in the degradation of sulfate lignin and many lignin model compounds makes it a potential candidate for the management of lignin produced as waste from the biorefinery and pulp and paper industries (Figure 4).

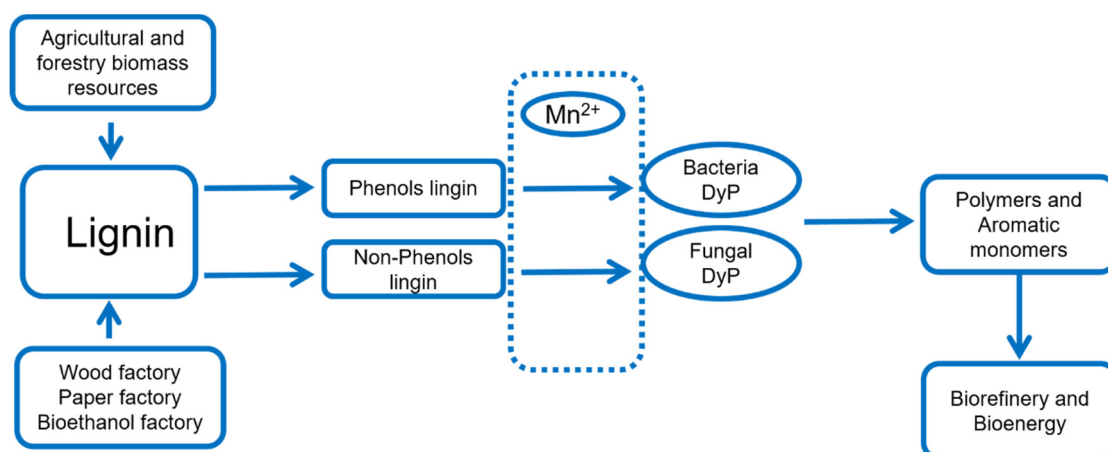


Figure 4. Process graph shows the possible research direction of DyPs in lignin and it shows that bacteria prefer to use phenolic lignin, while fungi prefer non-phenolic lignin.

3.2. Dye Decolorization

Textile printing and dyeing wastewater has always been regarded as the most challenging industrial wastewater due to its large water volume, deep color, and high concentration of organic matter. An important factor that makes handling difficult is that it contains various types of dyes, most of which contain aromatic ring structures and are biologically toxic [50]. The treatment methods of dye wastewater mainly include a physical, chemical, and biological method. The biological method has no secondary pollution and low cost, and it has always been the focus of dye wastewater treatment research [51]. At present, there have been reports on DyPs on azo dyes, anthraquinone dyes, and triarylmethane dyes, especially anthraquinone dyes. DyPs have different decolorization effects on different types of dyes [52]. This difference is often due to the difference in the ability of electron donor substituents on the aromatic ring of the dye to absorb electrons. The DyP decolorization efficiency of different strains also showed great differences. For example, Colpa et al. found that under the condition of pH 3.0, TfuDyP derived from *Thermobifida fusca* reacted for one hour to Eosin Y, Acid Blue 129, and Crocetin. The decolorization rate of Reactive Blue 14 and Reactive Blue 19 both exceeded 80%, but the decolorization rate of Reactive Blue 14 and Reactive Blue 19 was less than 60% at 1 h, and the decolorization rate of Reactive Blue 19 by BaD DyP from *T. cucumeris* Dec reached 80% in 24 h of reaction [20,21,32]. To choose the dye substrates, DyPs usually have a higher degradation effect on anthraquinone dyes but showed greater differences in other types of dyes such as BsDyP, PpDyP, and azo reductase. In the degradation effect of PpAzoR and laccase CotA on a variety of dyes, it was observed that the decolorization rate of BsDyP and PpDyP on the anthraquinone dyes Reactive Blue 5, Reactive Blue 19, and Acid Blue 5 reached more than 60%. The difference in decolorization rate was slight, while the decolorization rate of PpAzoR and laccase CotA to the above dyes is less than 20%. In addition, when decolorizing azo dyes, BsDyP and PpDyP showed that the decolorization rate of PpDyP on the azo dye Acid Red 299 reached 80%, while the decolorization rate of BsDyP was only 20%.

On the contrary, the decolorization efficiency of Direct Red R, BsDyP reached 76%, while PpDyP was only 18% [26,53]. After the cultivation, the mixed and fermented laccase-producing *B. odysseyi* SUK3, *B. cereus* EBT1 and other strains obtained laccase, azo reductase, and other enzymes. When the dye was decolorized, the decolorization about the Red M5B effect was far better than laccase treatment alone [54]. Moreover, it was observed that although certain enzymes can have broader specificity to dye materials, the product after transformation was more toxic than the dye itself, such as the azo reductase PpAzoR of *P. putida*. However, when the laccase CotA was added to the wastewater treated by PpAzoR, the toxicity was reduced when the two genes were co-expressed in *E. coli*.

The decolorization level of the recombined bacteria was unchanged compared with the previous one, but the detoxification level was increased by 50% [55]. At present, there are few reports about the cooperative treatment of wastewater by multiple enzymes based on DyP. However, given the unique advantages of DyP, it still provides a greater possibility for DyP treatment of textile printing and dyeing wastewater.

It is well known that DyPs have efficient degradation effects on anthraquinone dyes, especially C and D-Type DyP [20]. For azo, triphenylmethane, and other dyes, they show different degradation efficiency. Therefore, there are some studies on the degradation mechanism of anthraquinone dyes. Reactive Blue 5 and Reactive Blue 19 are typical structures of anthraquinone dye sand. BAD DyP can degrade Reactive Blue 5 by cleaving an anthraquinone framework [56,57]. A unique hydrolase mechanism has been proposed, which uses H_2O released by peroxidase function to exert hydrolase activity during the degradation of anthrone (Figure 5A) [58]. In addition, there is another theory that the reaction is carried out through the traditional peroxidase catalytic pathway, and anthrone can be spontaneously hydrolyzed when it exists as an intermediate of anthraquinone (Figure 5B) [59]. The first theory is more convincing because it was found in subsequent studies that although horseradish peroxidase and VP enzymes produced by *Pseudomonas amygdala* can also decolorize Reactive Blue 5, the presence of phthalic acid was not detected in the final results, indicating that the catalytic mechanism of these two enzymes is different from BadDyP, and illustrates two understanding processes of Reactive Blue 5 and the pyrolysis process (Figure 5) [56].

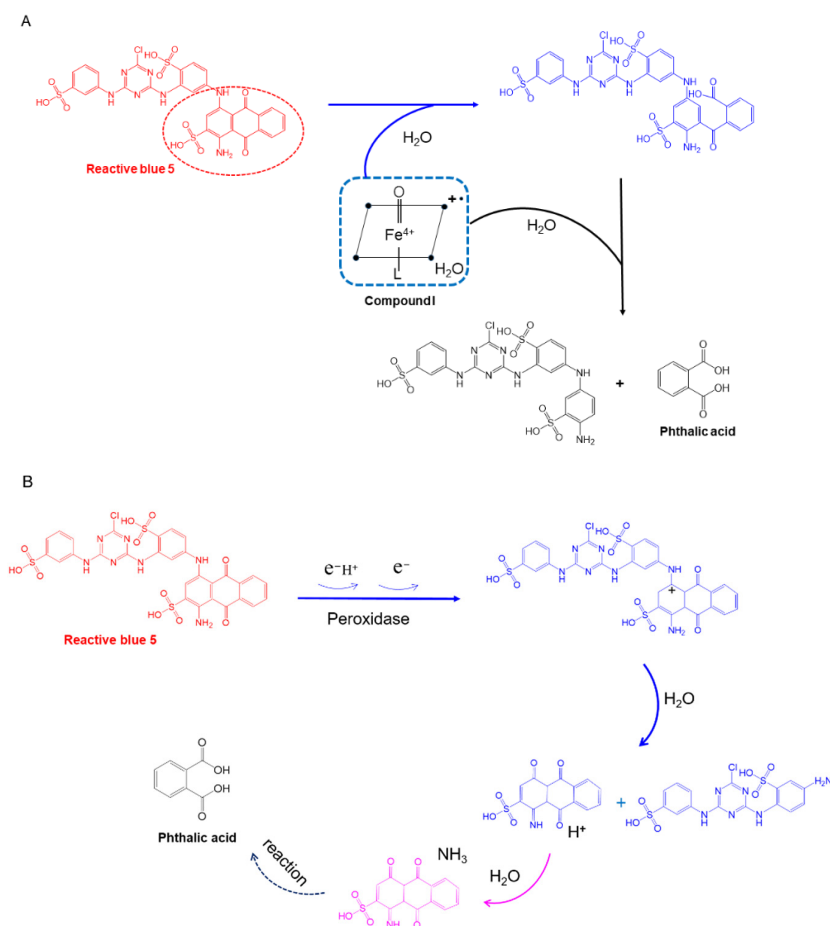


Figure 5. Two degradation mechanisms of reactive anthraquinone dyes. The red dotted circle represents anthrone, the basic functional group of anthraquinone dyes. **(A)** Mechanism of hydrolase reaction. **(B)** Mechanism of peroxidase reaction (HRP).

Industrial products with dye stuff are everywhere in our lives, the most common ones being in the clothes we wear and are also contained in a large number of other textile and chemical fiber products. The world produces millions of tons of textile waste every year. The three countries with the highest production of textile waste are the United States (15.1 million tons), China (2.6 million tons), and Britain (1.7 million tons). The annual treatment of textile waste consumes a lot of energy and money. Some studies have shown that textile waste can become a biomass source for the production of value-added products and renewable energy [60]. Acid hydrolysis and laser methods are often used in the decolorization pretreatment. At the same time as the degradation of dyes, nitric acid treatment and pyrolysis products will still consume energy.

Moreover, the wild-type DyP usually expresses a high activity under acidic conditions and the enzyme itself was still a protein after its function. The protein hydrolysate can be used for microbial growth medium or biological fertilizer, or animal feed, which is conducive to the development of a circular economy [61]. It has been mentioned that DyP has a high redox potential. It may be that the pretreatment process or composite enzyme treatment process combined with an acid and an enzyme in the decolorization process may have unpredictable benefits for the utilization of waste compounds (Figure 6). Recycled fiber has a broad market in 3D printing and material applications. Although there is no research on DyP in this field, I think it is a meaningful research direction of DyP in the recycling economy system, which will produce substantial economic benefits and slow down the environmental problems.

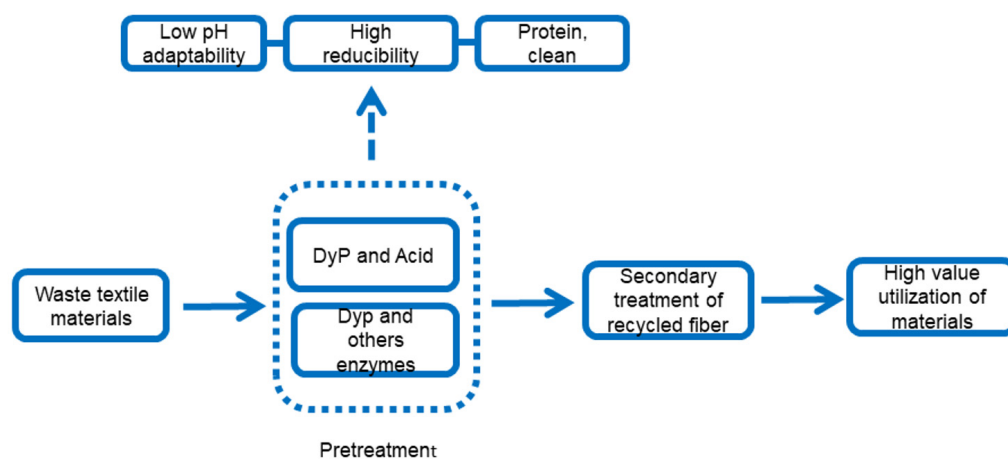


Figure 6. Process graph shows the possible research direction on DyPs regarding dye utilization.

3.3. Other Potential Applications

DyPs had a wide range of substrates and strong acid resistance and can play a stable function in halogenation, epoxidation, hydroxylation, and other reactions. It became a research hotspot in papermaking, coatings, environmental protection, medical, bioenergy, and other industries. In addition to the efficient decolorization of anthraquinone dyes and degradation of certain lignin substrates, it can also be used in food and medicine. Scheibner et al. found that one of the fungal enzymes, DyP-type peroxidase, can effectively degrade β -carotene. β -carotene is a yellow fat-soluble compound. It is a natural pigment that stably exists in nature. It can effectively degrade β -carotene and whiten foods and beverages containing whey [62]. At present, the corresponding DyP has been patented and sold by DSM.

Similarly, in 2020, Krahe identified a new type of DyP PsaPOX produced by *Pleurotus sapidus* with an olefin degrading ability, which can crack arylalkenes (E)-methyl isoeugenol, α -methylstyrene, and *trans*-anethole. The cleavage products such as anisaldehyde, as Spice additives, are widely used in the food industry [16]. In addition, due to the significant increase in drug resistance and pathogenic bacteria, it is urgent to discover new targeted

antibacterial drugs. The advantage of the DyPs enzyme is that it is very abundant in the bacterial proteome, including many pathogenic bacteria. These enzymes do not exist in mammals, indicating that the DyPs enzyme may become a new type of targeted antibacterial drug. However, peroxidase produced by *P. fluorescens* GcM5-1A has substantial pathological toxicity to the cells of Japanese black pine, which provides a possibility for the development of targeted antibacterial drugs [35]. In cosmetic applications, Shin et al. combined the laccase (CueO) produced by *Escherichia coli* with DyP produced by *Bacillus subtilis* and the dockerin domain of *Clostridium cellulovorans* endoglucanase B to form a complex enzyme that can effectively reduce keratinocytes. Compared with pure laccase, the number of melanin particles increased the specific binding of melanin by 64%, and the degradation efficiency is 6.4 times higher than that of the former. As a new generation of whitening additives, it has a great industrial application potential [39]. The research on the DyP biosensor, such as hydrogen peroxide biosensor, DyP has a unique advantage. In 2020, Barbosa used the defective strain *P. putida* MET94 as the basis, and direct evolution produced three isomers of PpDyP. They also successfully developed a biosensor for detecting hydrogen peroxide content through immobilization technology and analyzed its stability and sensitivity through electrochemical technology. Compared with traditional bioelectrodes, the sensitivity is increased 10–10⁴ times [32]. At present, the scope of applications of DyPs was relatively limited. Still, perhaps in the future, DyPs may achieve results that those other peroxidases cannot achieve because of their unique advantages.

4. New Technology Promotes DyP Industrialization (Application) Research

As mentioned above, DyP has a wide range of application values. Still, its unique properties also limit its industrial application, such as low yield, low pH adaptation, high production cost, and so on. With the development of *dypase* genomic data mining, synthetic biology technology has developed rapidly, which may accelerate the industrial application of DyPs (Figure 7).



Figure 7. The industrial applications of DyPs.

4.1. Improvement of DyPs Properties by Gene-Editing Technology

The practical application of DyPs is subject to the influence of environmental factors. At the same time, the enzyme activity is low, and the pH range is small, limiting the practical application of DyPs. The development of directed evolution technology and

gene recombination technology provides unlimited possibilities for solving the practical application of DyP. The construction of a gene database and phylogenetic analysis revealed the omics relationship between DyPs, and gene functions have been elucidated. It indicated that the research on DyPs could reach a new stage using molecular biology [57,63]. DyPs can maintain a high activity in acidic conditions and tend to express high activity at an acidic pH to degrade lignin substrates. However, the pH of the water used in the paper mill and the wastewater of the printing and dyeing plant is alkaline. Improving the enzyme activity of DyP provides a new method to solve the practical application of DyP.

In 2014, Yu et al. [37] cloned a DyP-type peroxidase gene SVIDIP from the gene library of *Saccharomonospora viridis* with a sequence similar to the peroxidase of the dye decolorizing microorganism. The protein can efficiently decolorize triarylmethane dyes, anthraquinone dyes, and azo dyes under neutral to alkaline conditions. The optimum pH of the reconstituted SviDyP was 7.0 and the optimum temperature is 70 °C. In addition, compared with other DyPs, it has a wide range of alkali resistance (pH 4.0–9.0) and heat resistance (37–80 °C). The actual application process can accelerate the bleaching effect of eucalyptus kraft pulp, the kappa number reduced by 21.8%, and the whiteness is increased by 2.98%. These excellent characteristics make sviDyP peroxidase a beneficial enzyme in the pulp and paper industry [36]. At the same time, directed evolution and modification of strains are also widely used in DyP-producing strains. Based on *P. putida* MET94, evolution was directed towards a mutant strain *P. putida* 6E10 with the three mutant genes E188K, A142V, and H125Y. The oxidation performance of the mutants on eugenylphenols, GGE, and sulfate lignin, has been greatly improved, and even the catalytic efficiency of 2,6-dimethoxyphenol has been increased 100 times. At the same time, unlike the DyP produced by the wild-type strain, the recombinant PpDyP prefers to participate in the reaction at pH 8.5, which greatly improves the pH resistance [32].

Pour et al. applied a directed evolution technology to dye the peroxidase Dyp1B of *P. fluorescens* Pf-5, and saturation mutagenesis was used to generate a focused library on the seven active site residues near the heme cofactor. The reaction rate of *P. fluorescens* N193L and *P. fluorescens* H169L mutants to DCP (2,6-dichlorophenol) increased 7–8 times. The mutant *P. fluorescens* S223N and *P. fluorescens* H127R showed that the oxidation rate of manganese (ii) was increased by 4–7 times. Compared with wild Dyp1B, mutant *P. fluorescens* H169L showed a stronger product release ability to alkali lignin. The vanillin content in the product increased significantly, indicating a brighter prospect in the biorefinery of lignin [47]. The technology of the directed evolution of enzymes is also constantly innovating. Abdulrahman took the lead in using the bacterial extracellular protein secretion (BENNY) system, which realized the evolution of DyP simply and efficiently and accelerated the protein production of DyP4 of *Pleurotus ostreatus* strain PC15 [64]. The Retrofit and excavation of the high degradability DyPs indicated that DyP could be used as a pretreatment process in the biorefinery of lignin, resulting in the presence of a large number of aromatic monomers during the degradation of lignin. For example, in Germany, the active modification of *Amycolatopsis* sp. ATCC 39116 and *Amycolatopsis* sp. ATCC39116 was used as the cell factory to realize the efficient conversion of guaiacol cis-mucoid, along with DyP, showing the potential to crack lignin to generate a large amount of guaiacol [65]. Another aspect of the impact of gene-editing technology on DyP is that, based on elucidating the degradation mechanism, the metabolic pathways of DyP-producing strains are actively modified to complete the targeted production of the final products.

4.2. Choose Suitable Host Cells to Promote the Industrial Application of Enzymes

DyP-producing microorganisms, especially fungal microorganisms, have a long incubation period during the enzyme production process, which means that the production cost of DyP is high. The high cost means that DyP does not seem suitable for large-scale industrial production. Similar to other enzymes, choosing a suitable host cell as the chassis cell, combined with a mature high-density fermentation process, needs a breakthrough. At present, in the application of industrial enzymes, a large number of unmodified or

modified recombinant enzymes have been produced through heterologous expression systems to deal with the problems in practical applications [66]. In the peroxidase family, the production of MnP and LiP using insect cells and a Bacillus virus expression system was first reported in 1991, but there are disadvantages of low yield and high cost [67,68]. Gelpke et al. used white-rot fungus as an expression vector to produce MnP and Lip, and the purified LiP content reached 2 mg/L [69]. Tsukihara et al. used *Pleurotus ostreatus* as a carrier to bring in the MnP2 gene, and the output of MnP2 reached 21 mg/L after expression [70]. However, homologous expression requires extensive strains screening, and the natural enzymes produced can also contaminate the recombinant enzymes. *E. coli* model bacteria have been widely used as fungal enzyme expression platforms. Many recombinant enzymes have been successfully isolated from inclusion bodies. The purification efficiency in vitro can reach 28%, and the maximum yield is 1.5–14 mg/L [71]. To increase the stability of the expression of many fungal enzymes, some fungal and yeast expression systems are often used for post-translational modification and post-translational modification. In addition to LiP and MnP, DyP can also be expressed on different exogenous platforms. Using *Escherichia coli* as an expression vector to construct engineered bacteria, the DyP yield increased from wild-type 0.1 mg/L to 63 mg/L [72]. The DyP expression genes that have been identified that can be stably expressed in *E. coli* are mainly from *Thermus thermophilus*, *Pseudomonas aeruginosa*, *P. putida*, *B. subtilis*, and *Chloromonospora*, *P. fluorescens*, and *Rhodococcus* RHA1. Such recombinantly expressed enzymes are widely used in the degradation of dyes and more complex lignin substrates. To obtain more efficient enzyme production, as the most commonly used protein expression system, the recombinant *E. coli* expression system is superior to other expression systems [64]. The most widely used for recombinant protein expression in *E. coli* BL21 (DE3) and its derivative strains. The currently commonly used expression plasmid results from multiple replicons, promoters, selectable markers, multiple cloning sites, and fusion protein removal strategies. The change and regulation of macroscopic variables such as pH, dissolved oxygen, oxygen consumption rate, carbon dioxide release rate, respiratory quotient, bacterial cell growth, sugar consumption, and nitrogen consumption are important guarantees for the industrialization of *E. coli* expression systems. The expression level of the *E. coli* metabolic pathway genes has important implications for the aforementioned studies. Guide meaning [73]. Various eukaryotic expression systems have emerged, but recombinant *E. coli* is still a powerful tool for basic research and commercial production of recombinant proteins and biochemical products due to its many advantages. In the field of producing DyPs, the expression of ZmdyP, BaDyP, AajDyP, eDyP, and SvidDyP has been achieved and has shown high stability. The *E. coli* expression system will play a greater role in experimental research and industrial production applications [33,74–76].

4.3. The Rise of Synthetic Protein Technology

Although DyPs have great application potential in industry, environment, food, medicine, etc., the separation and purification of DyPs from *E. coli* or other strains are still very time-consuming. These shortcomings often limit the practical application of DyPs. With the elucidation of the structure of more and more DyP family enzymes, researchers are studying the structure of DyPs and have found that building the structure of DyPs based on metalloenzymes can better clarify the structure and function of natural enzymes. At the same time, inspired by the characteristic amino acid residues of DyP, such as Tyr and Trp, it is possible to artificially design and construct functional enzymes of DyP [76]. At present, many oxidases and reductases have been artificially synthesized. Peroxidase contains heme protein. The biological functions of heme protein include oxygen transfer (hemoglobin, HB, and myoglobin, MB), electron transfer (cytochrome C, CytC), and catalysis (peroxidase and cell Pigment P450) [77]. Lin et al. engineered Tyr/Trp in the heme center, using MB as a protein scaffold, and designed an artificial DyP to degrade industrial dyes [78]. Yan et al. introduced a distal Tyr at position 43 (F43Y mutation) of sperm whale Mb, which resulted in the spontaneous formation of a new Tyr-heme crosslink between the hydroxyl group at

Tyr43 and the 4-vinyl group of heme, which not only increased the stability of the protein but also improved the activity of peroxidase, which proves that F43Y can be used as an ideal protein scaffold for artificial DyPs [79]. At the same time, a second distal Tyr was introduced into F43 MB in the I107 mutation, and its recombined dye decolorizing ability was 2.4 times higher than that of F43Y Mb and 17.7 times higher than that of the wild type. Immediately, Li et al. introduced a remote Trp at position 138 of MB. Its catalytic efficiency was 20 and 144 times higher than that of the F43Y MB wild-type. It is worth noting that its activity is 4.3 times higher than VcDyP produced by *Vibrio cholerae* [80].

When the theory of using MB as a protein scaffold was recognized and promoted, Warren et al. found that artificially designing Trp residues in cytochrome C peroxidase (CcP) can significantly improve its ability to oxidize dyes. The method is to introduce two Trp residues (A193W and Y229W) in combination with natural W191 to form an artificial Trp wire-mounted structure on the surface of heme and protein, thereby promoting the jump of electrons from the active site to the surface of the protein and speeding up the redox reaction. The double mutant A193W/Y229W Ccp's oxidation rate was significantly higher than the single mutant and wild type. Other types of peroxidases can also be formed through the modification of DyP. For example, DyP can be converted into DHP (dehaloperoxidase) through protein engineering. Bugg et al. [50] used directed evolution to enhance the oxidation activity of DyP1B on phenolic substrates. They found that the two mutations, N193L and H169L, of DyPs1B increased the catalytic efficiency of 2,6-dichlorophenol by more than 8 times and possessed DHP enzyme capacity [47]. The artificial design of DyP provides more possibilities for the industrial utilization of Dyps enzymes.

5. Prospective

Although domestic research on dye decoloring peroxidase is relatively late, DSM has quickly developed corresponding enzyme products for the food industry. With the rise of recombination technology, directed evolution technology, and artificial synthesis technology, more and more recombinases with alkali resistance, high-temperature resistance, and high catalytic efficiency will be used in the pulp and paper industry, advanced biofuels, and in the treatment of wastewater. Dye decolorizing enzymes have attracted wide attention because of their high oxidative properties, acid resistance, rich resources, and easy expression in industrial host organisms.

At present, the structure of some dye-decoloring peroxidase enzymes is clear, and the enzymatic properties of dye-decoloring peroxidase enzymes have also been studied. However, there is still a long way to go before the real industrial application. To overcome the problem that restricts the industrialization process of dye decoloring enzymes, it was suggested to follow certain aspects. Firstly, we must understand the specific mechanism of DyP in lignin degradation and dye decolorization and explore the efficient degradation in practical applications. For efficient enzymes, we must select high-degrading DyPs through the metagenomic library. Secondly, it is necessary to achieve high-efficiency secretion and expression of DyP in a heterologous host and increase the output of DyP as much as possible. On this basis, it can also be considered to achieve cooperative co-expression with other enzymes or directed evolution to recombine DyP to make the enzyme work better. In addition, DyPs can be artificially modified or constructed through chemical engineering and protein engineering to obtain more efficient enzymes. Finally, we must make full use of enzymatic technology to improve the reproducibility and stability of DyP. Perhaps with the improvement of the catalytic efficiency of DyP, the increase of production, and the enhancement of alkali resistance and toxicity, the industrial application of DyP will be promising, and it will have remarkable potential in the future.

Supplementary Materials: The following are available online at <https://www.mdpi.com/article/10.3390/catal11080955/s1>; Table S1: Describes the different types and specific characteristics of DyPs isolated from various bacterial strains.

Author Contributions: D.Z. conceptualized the review, L.X. wrote the manuscript, M.A.Q. and J.S. prepared the figures and tables, D.Z., L.X., J.S., M.A.Q. and L.G. reviewed and edited the manuscript. All authors have read and agreed to the published version of the manuscript.

Funding: The authors are thankful for the financial support of the National Key R&D Program of China (Grant No.2018YFE0107100) and the Priority Academic Program Development of Jiangsu Higher Education Institutions.

Institutional Review Board Statement: Not applicable.

Informed Consent Statement: Not applicable.

Conflicts of Interest: The authors declare no conflict of interest.

References

1. Davies, M.J.; Hawkins, C.L.; Pattison, D.I.; Rees, M.D. Mammalian heme peroxidases: From molecular mechanisms to health implications. *Antioxid. Redox Signal.* **2008**, *10*, 1199–1234. [[CrossRef](#)] [[PubMed](#)]
2. Heinfling, A.; Martínez, M.A.J.; Martínez, A.T.; Bergbauer, M.; Szewzyk, U. Purification and characterization of peroxidases from the dye-decolorizing fungus *Bjerkandera adusta*. *FEMS Microbiol. Lett.* **1998**, *165*, 43–50. [[CrossRef](#)]
3. Sugano, Y.; Muramatsu, R.; Ichiyangi, A.; Sato, T.; Shoda, M. DyP, a unique dye-decolorizing peroxidase, represents a novel heme peroxidase family: ASP171 replaces the distal histidine of classical peroxidases. *J. Biol. Chem.* **2007**, *282*, 36652–36658. [[CrossRef](#)]
4. Yoshida, T.; Sugano, Y. A structural and functional perspective of DyP-type peroxidase family. *Arch. Biochem. Biophys.* **2015**, *574*, 49–55. [[CrossRef](#)] [[PubMed](#)]
5. Kim, S.J.; Shoda, M. Purification and characterization of a novel peroxidase from *Geotrichum candidum* dec 1 involved in decolorization of dyes. *Appl. Environ. Microbiol.* **1999**, *65*, 1029–1035. [[CrossRef](#)] [[PubMed](#)]
6. Hofrichter, M.; Ullrich, R.; Pecyna, M.J.; Liers, C.; Lundell, T. New and classic families of secreted fungal heme peroxidases. *Appl. Microbiol. Biotechnol.* **2010**, *87*, 871–897. [[CrossRef](#)] [[PubMed](#)]
7. Singh, S.; Pandey, V.P.; Naaz, H.; Dwivedi, U.N. Phylogenetic analysis, molecular modeling, substrate-inhibitor specificity, and active site comparison of bacterial, fungal, and plant heme peroxidases. *Biotechnol. Appl. Biochem.* **2012**, *59*, 283–294. [[CrossRef](#)] [[PubMed](#)]
8. Zámocký, M. Phylogenetic relationships in class I of the superfamily of bacterial, fungal, and plant peroxidases. *Eur. J. Biochem.* **2004**, *271*, 3297–3309. [[CrossRef](#)] [[PubMed](#)]
9. Veitch, N.C. Horseradish peroxidase: A modern view of a classic enzyme. *Phytochemistry* **2004**, *65*, 249–259. [[CrossRef](#)] [[PubMed](#)]
10. Yoshida, T.; Tsuge, H.; Konno, H.; Hisabori, T.; Sugano, Y. The catalytic mechanism of dye-decolorizing peroxidase DyP may require the swinging movement of an aspartic acid residue. *FEBS J.* **2011**, *278*, 2387–2394. [[CrossRef](#)]
11. Brown, M.E.; Barros, T.; Chang, M.C. Identification and characterization of a multifunctional dye peroxidase from a lignin-reactive bacterium. *ACS Chem. Biol.* **2012**, *7*, 2074–2081. [[CrossRef](#)] [[PubMed](#)]
12. Ogola, H.J.; Kamiike, T.; Hashimoto, N.; Ashida, H.; Ishikawa, T.; Shibata, H.; Sawa, Y. Molecular characterization of a novel peroxidase from the cyanobacterium *Anabaena* sp. strain PCC 7120. *Appl. Environ. Microbiol.* **2009**, *75*, 7509–7518. [[CrossRef](#)] [[PubMed](#)]
13. Salvachúa, D.; Prieto, A.; Martínez, Á.T.; Martínez, M.J. Characterization of a novel dye-decolorizing peroxidase (DyP)-type enzyme from *Irpex lacteus* and its application in enzymatic hydrolysis of wheat straw. *Appl. Environ. Microbiol.* **2013**, *79*, 4316–4324. [[CrossRef](#)]
14. Lauber, C.; Schwarz, T.; Nguyen, Q.K.; Lorenz, P.; Lochnit, G.; Zorn, H. Identification, heterologous expression and characterization of a dye-decolorizing peroxidase of *Pleurotus sapidus*. *AMB Express* **2017**, *7*, 164. [[CrossRef](#)] [[PubMed](#)]
15. Liers, C.; Pecyna, M.J.; Kellner, H.; Worrlich, A.; Zorn, H.; Steffen, K.T.; Hofrichter, M.; Ullrich, R. Substrate oxidation by dye-decolorizing peroxidases (DyPs) from wood- and litter-degrading agaricomycetes compared to other fungal and plant heme-peroxidases. *Appl. Microbiol. Biotechnol.* **2013**, *97*, 5839–5849. [[CrossRef](#)]
16. Krahe, N.K.; Berger, R.G.; Ersoy, F. A DyP-Type Peroxidase of *Pleurotus sapidus* with Alkene Cleaving Activity. *Molecules* **2020**, *25*, 1536. [[CrossRef](#)] [[PubMed](#)]
17. Contreras, H.; Joens, M.S.; McMath, L.M.; Le, V.P.; Tullius, M.V.; Kimmey, J.M.; Bionghi, N.; Horwitz, M.A.; Fitzpatrick, J.A.; Goulding, C.W. Characterization of a Mycobacterium tuberculosis nanocompartment and its potential cargo proteins. *J. Biol. Chem.* **2014**, *289*, 18279–18289. [[CrossRef](#)] [[PubMed](#)]
18. Létoffé, S.; Heuck, G.; Delepelaire, P.; Lange, N.; Wandersman, C. Bacteria capture iron from heme by keeping tetrapyrrol skeleton intact. *Proc. Natl. Acad. Sci. USA* **2009**, *106*, 11719–11724. [[CrossRef](#)] [[PubMed](#)]
19. Liu, X.; Du, Q.; Wang, Z.; Zhu, D.; Huang, Y.; Li, N.; Wei, T.; Xu, S.; Gu, L. Crystal structure and biochemical features of EfeB/YcdB from *Escherichia coli* O157: ASP235 plays divergent roles in different enzyme-catalyzed processes. *J. Biol. Chem.* **2011**, *286*, 14922–14931. [[CrossRef](#)] [[PubMed](#)]
20. Colpa, D.I.; Fraaije, M.W.; van Bloois, E. DyP-type peroxidases: A promising and versatile class of enzymes. *J. Ind. Microbiol. Biotechnol.* **2014**, *41*, 1–7. [[CrossRef](#)] [[PubMed](#)]

21. Zámocký, M.; Hofbauer, S.; Schaffner, I.; Gasselhuber, B.; Nicolussi, A.; Soudi, M.; Pirker, K.F.; Furtmüller, P.G.; Obinger, C. Independent evolution of four heme peroxidase superfamilies. *Arch. Biochem. Biophys.* **2015**, *574*, 108–119. [[CrossRef](#)] [[PubMed](#)]
22. Zubieta, C.; Krishna, S.S.; Kapoor, M.; Kozbial, P.; McMullan, D.; Axelrod, H.L.; Miller, M.D.; Abdubek, P.; Ambing, E.; Astakhova, T.; et al. Crystal structures of two novel dye-decolorizing peroxidases reveal a beta-barrel fold with a conserved heme-binding motif. *Proteins* **2007**, *69*, 223–233. [[CrossRef](#)]
23. Singh, R.; Eltis, L.D. The multihued palette of dye-decolorizing peroxidases. *Arch. Biochem. Biophys.* **2015**, *574*, 56–65. [[CrossRef](#)] [[PubMed](#)]
24. Rai, A.; Klare, J.P.; Reinke, P.Y.; Englmaier, F.; Fohrer, J.; Fedorov, R.; Taft, M.H.; Chizhov, I.; Curth, U.; Plettenburg, O. Structural and Biochemical Characterization of a Dye-Decolorizing Peroxidase from *Dictyostelium discoideum*. *Int. J. Mol. Sci.* **2021**, *22*, 6265. [[CrossRef](#)] [[PubMed](#)]
25. Chen, C.; Shrestha, R.; Jia, K.; Gao, P.F.; Geisbrecht, B.V.; Bossmann, S.H.; Shi, J.; Li, P. Characterization of Dye-decolorizing Peroxidase (DyP) from *Thermomonospora curvata* Reveals Unique Catalytic Properties of A-type DyPs. *J. Biol. Chem.* **2015**, *290*, 23447–23463. [[CrossRef](#)] [[PubMed](#)]
26. Santos, A.; Mendes, S.; Brissos, V.; Martins, L.O. New dye-decolorizing peroxidases from *Bacillus subtilis* and *Pseudomonas putida* MET94: Towards biotechnological applications. *Appl. Microbiol. Biotechnol.* **2014**, *98*, 2053–2065. [[CrossRef](#)] [[PubMed](#)]
27. Rahmanpour, R.; Rea, D.; Jamshidi, S.; Fülöp, V.; Bugg, T.D. Structure of *Thermobifida fusca* DyP-type peroxidase and activity towards Kraft lignin and lignin model compounds. *Arch. Biochem. Biophys.* **2016**, *594*, 54–60. [[CrossRef](#)] [[PubMed](#)]
28. Azevedo, A.M.; Martins, V.C.; Prazeres, D.M.; Vojinović, V.; Cabral, J.M.; Fonseca, L.P. Horseradish peroxidase: A valuable tool in biotechnology. *Biotechnol. Annu. Rev.* **2003**, *9*, 199–247. [[CrossRef](#)] [[PubMed](#)]
29. Ahmad, M.; Roberts, J.N.; Hardiman, E.M.; Singh, R.; Eltis, L.D.; Bugg, T.D. Identification of DypB from *Rhodococcus jostii* RHA1 as a lignin peroxidase. *Biochemistry* **2011**, *50*, 5096–5107. [[CrossRef](#)]
30. Shrestha, R.; Chen, X.; Ramyar, K.X.; Hayati, Z.; Carlson, E.A.; Bossmann, S.H.; Song, L.; Geisbrecht, B.V.; Li, P. Identification of Surface-Exposed Protein Radicals and A Substrate Oxidation Site in A-Class Dye-Decolorizing Peroxidase from *Thermomonospora curvata*. *ACS Catal.* **2016**, *6*, 8036–8047. [[CrossRef](#)]
31. Singh, R.; Grigg, J.C.; Armstrong, Z.; Murphy, M.E.P.; Eltis, L.D. Distal heme pocket residues of B-type dye-decolorizing peroxidase: Arginine but not aspartate is essential for peroxidase activity. *J. Biol. Chem.* **2012**, *287*, 10623–10630. [[CrossRef](#)] [[PubMed](#)]
32. Barbosa, C.; Silveira, C.M.; Silva, D.; Brissos, V.; Hildebrandt, P.; Martins, L.O.; Todorovic, S. Immobilized dye-decolorizing peroxidase (DyP) and directed evolution variants for hydrogen peroxide biosensing. *Biosens. Bioelectron.* **2020**, *153*, 112055. [[CrossRef](#)] [[PubMed](#)]
33. Liu, X.; Yuan, Z.; Wang, J.; Cui, Y.; Liu, S.; Ma, Y.; Gu, L.; Xu, S. Crystal structure and biochemical features of dye-decolorizing peroxidase YfeX from *Escherichia coli* O157 Asp(143) and Arg(232) play divergent roles toward different substrates. *Biochem. Biophys. Res. Commun.* **2017**, *484*, 40–44. [[CrossRef](#)] [[PubMed](#)]
34. Cao, J.; Woodhall, M.R.; Alvarez, J.; Cartron, M.L.; Andrews, S.C. EfeUOB (YcdNOB) is a tripartite, acid-induced and CpxAR-regulated, low-pH Fe²⁺ transporter that is cryptic in *Escherichia coli* K-12 but functional in *E. coli* O157:H7. *Mol. Microbiol.* **2007**, *65*, 857–875. [[CrossRef](#)]
35. Kong, L.; Guo, D.; Zhou, S.; Yu, X.; Hou, G.; Li, R.; Zhao, B. Cloning and expression of a toxin gene from *Pseudomonas fluorescens* GcM5-1A. *Arch. Microbiol.* **2010**, *192*, 585–593. [[CrossRef](#)] [[PubMed](#)]
36. Yu, W.; Liu, W.; Huang, H.; Zheng, F.; Wang, X.; Wu, Y.; Li, K.; Xie, X.; Jin, Y. Application of a novel alkali-tolerant thermostable DyP-type peroxidase from *Saccharomonospora viridis* DSM 43017 in biobleaching of eucalyptus kraft pulp. *PLoS ONE* **2014**, *9*, e110319. [[CrossRef](#)] [[PubMed](#)]
37. Min, K.; Gong, G.; Woo, H.M.; Kim, Y.; Um, Y. A dye-decolorizing peroxidase from *Bacillus subtilis* exhibiting substrate-dependent optimum temperature for dyes and β-ether lignin dimer. *Sci. Rep.* **2015**, *5*, 8245. [[CrossRef](#)] [[PubMed](#)]
38. Field, M.J.; Bains, R.K.; Warren, J.J. Using an artificial tryptophan “wire” in cytochrome c peroxidase for oxidation of organic substrates. *Dalton Trans.* **2017**, *46*, 11078–11083. [[CrossRef](#)] [[PubMed](#)]
39. Shin, S.K.; Hyeon, J.E.; Joo, Y.C.; Jeong, D.W.; You, S.K.; Han, S.O. Effective melanin degradation by a synergistic laccase-peroxidase enzyme complex for skin whitening and other practical applications. *Int. J. Biol. Macromol.* **2019**, *129*, 181–186. [[CrossRef](#)]
40. Ralph, J.; Lapierre, C.; Boerjan, W. Lignin structure and its engineering. *Curr. Opin. Biotechnol.* **2019**, *56*, 240–249. [[CrossRef](#)] [[PubMed](#)]
41. Janusz, G.; Pawlik, A.; Sulej, J.; Swiderska-Burek, U.; Jarosz-Wilkolazka, A.; Paszczynski, A. Lignin degradation: Microorganisms, enzymes involved, genomes analysis and evolution. *FEMS Microbiol. Rev.* **2017**, *41*, 941–962. [[CrossRef](#)]
42. Zhu, D.; Zhang, P.; Xie, C.; Zhang, W.; Sun, J.; Qian, W.J.; Yang, B. Biodegradation of alkaline lignin by *Bacillus ligninophilus* L1. *Biotechnol. Biofuels* **2017**, *10*, 44. [[CrossRef](#)] [[PubMed](#)]
43. Xiao, J.; Zhang, S.; Chen, G. Mechanisms of Lignin-Degrading Enzymes. *Protein Pept. Lett.* **2020**, *27*, 574–581. [[CrossRef](#)]
44. Rajhans, G.; Sen, S.K.; Barik, A.; Raut, S. Elucidation of fungal dye-decolourizing peroxidase (DyP) and ligninolytic enzyme activities in decolourization and mineralization of azo dyes. *J. Appl. Microbiol.* **2020**, *129*, 1633–1643. [[CrossRef](#)]

45. Floudas, D.; Binder, M.; Riley, R.; Barry, K.; Blanchette, R.A.; Henrissat, B.; Martínez, A.T.; Otilar, R.; Spatafora, J.W.; Yadav, J.S.; et al. The Paleozoic origin of enzymatic lignin decomposition reconstructed from 31 fungal genomes. *Science* **2012**, *336*, 1715–1719. [[CrossRef](#)] [[PubMed](#)]
46. Kamimura, N.; Sakamoto, S.; Mitsuda, N.; Masai, E.; Kajita, S. Advances in microbial lignin degradation and its applications. *Curr. Opin. Biotechnol.* **2019**, *56*, 179–186. [[CrossRef](#)] [[PubMed](#)]
47. Rahman Pour, R.; Ehibhatioman, A.; Huang, Y.; Ashley, B.; Rashid, G.M.; Mendel-Williams, S.; Bugg, T.D.H. Protein engineering of *Pseudomonas fluorescens* peroxidase Dyp1B for oxidation of phenolic and polymeric lignin substrates. *Enzym. Microb. Technol.* **2019**, *123*, 21–29. [[CrossRef](#)] [[PubMed](#)]
48. Vanholme, R.; De Meester, B.; Ralph, J.; Boerjan, W. Lignin biosynthesis and its integration into metabolism. *Curr. Opin. Biotechnol.* **2019**, *56*, 230–239. [[CrossRef](#)]
49. Bugg, T.D.; Rahmanpour, R. Enzymatic conversion of lignin into renewable chemicals. *Curr. Opin. Chem. Biol.* **2015**, *29*, 10–17. [[CrossRef](#)] [[PubMed](#)]
50. Routoula, E.; Patwardhan, S.V. Degradation of Anthraquinone Dyes from Effluents: A Review Focusing on Enzymatic Dye Degradation with Industrial Potential. *Environ. Sci. Technol.* **2020**, *54*, 647–664. [[CrossRef](#)]
51. Piaskowski, K.; Świdowska-Dąbrowska, R.; Zarzycki, P.K. Dye Removal from Water and Wastewater Using Various Physical, Chemical, and Biological Processes. *J. AOAC Int.* **2018**, *101*, 1371–1384. [[CrossRef](#)]
52. Kaushik, P.; Malik, A. Fungal dye decolorization: Recent advances and future potential. *Environ. Int.* **2009**, *35*, 127–141. [[CrossRef](#)] [[PubMed](#)]
53. Mendes, S.; Brissos, V.; Gabriel, A.; Catarino, T.; Turner, D.L.; Todorovic, S.; Martins, L.O. An integrated view of redox and catalytic properties of B-type PpDyP from *Pseudomonas putida* MET94 and its distal variants. *Arch. Biochem. Biophys.* **2015**, *574*, 99–107. [[CrossRef](#)]
54. Kadam, A.A.; Kamatkar, J.D.; Khandare, R.V.; Jadhav, J.P.; Govindwar, S.P. Solid-state fermentation: Tool for bioremediation of adsorbed textile dyestuff on distillery industry waste-yeast biomass using isolated *Bacillus cereus* strain EBT1. *Environ. Sci. Pollut. Res. Int.* **2013**, *20*, 1009–1020. [[CrossRef](#)] [[PubMed](#)]
55. Mendes, S.; Farinha, A.; Ramos, C.G.; Leitão, J.H.; Viegas, C.A.; Martins, L.O. Synergistic action of azoreductase and laccase leads to maximal decolorization and detoxification of model dye-containing wastewaters. *Bioresour. Technol.* **2011**, *102*, 9852–9859. [[CrossRef](#)] [[PubMed](#)]
56. Linde, D.; Ruiz-Dueñas, F.J.; Fernández-Fueyo, E.; Guallar, V.; Hammel, K.E.; Pogni, R.; Martínez, A.T. Basidiomycete DyPs: Genomic diversity, structural-functional aspects, reaction mechanism and environmental significance. *Arch. Biochem. Biophys.* **2015**, *574*, 66–74. [[CrossRef](#)] [[PubMed](#)]
57. Sugano, Y.; Yoshida, T. DyP-Type Peroxidases: Recent Advances and Perspectives. *Int. J. Mol. Sci.* **2021**, *22*, 5556. [[CrossRef](#)] [[PubMed](#)]
58. Jones, P. Roles of water in heme peroxidase and catalase mechanisms. *J. Biol. Chem.* **2001**, *276*, 13791–13796. [[CrossRef](#)]
59. Sugano, Y.; Matsushima, Y.; Tsuchiya, K.; Aoki, H.; Hirai, M.; Shoda, M. Degradation pathway of an anthraquinone dye catalyzed by a unique peroxidase DyP from *Thanatephorus cucumeris* Dec 1. *Biodegradation* **2009**, *20*, 433–440. [[CrossRef](#)] [[PubMed](#)]
60. Asaadi, S.; Hummel, M.; Hellsten, S.; Härkäsalmi, T.; Ma, Y.; Michud, A.; Sixta, H. Renewable High-Performance Fibers from the Chemical Recycling of Cotton Waste Utilizing an Ionic Liquid. *Chem. Sus. Chem.* **2016**, *9*, 3250–3258. [[CrossRef](#)] [[PubMed](#)]
61. Navone, L.; Moffitt, K.; Hansen, K.A.; Blinco, J.; Payne, A.; Speight, R. Closing the textile loop: Enzymatic fibre separation and recycling of wool/polyester fabric blends. *Waste Manag.* **2020**, *102*, 149–160. [[CrossRef](#)]
62. Scheibner, M.; Hülsdau, B.; Zelena, K.; Nimtz, M.; de Boer, L.; Berger, R.G.; Zorn, H. Novel peroxidases of *Marasmius scorodionius* degrade beta-carotene. *Appl. Microbiol. Biotechnol.* **2008**, *77*, 1241–1250. [[CrossRef](#)]
63. Tian, J.H.; Pourcher, A.M.; Klingelschmitt, F.; Le Roux, S.; Peu, P. Class P dye-decolorizing peroxidase gene: Degenerated primers design and phylogenetic analysis. *J. Microbiol. Methods* **2016**, *130*, 148–153. [[CrossRef](#)]
64. Alessa, A.H.A.; Tee, K.L.; Gonzalez-Perez, D.; Omar Ali, H.E.M.; Evans, C.A.; Trevaskis, A.; Xu, J.H.; Wong, T.S. Accelerated directed evolution of dye-decolorizing peroxidase using a bacterial extracellular protein secretion system (BENNY). *Bioresour. Bioprocess.* **2019**, *6*, 20. [[CrossRef](#)] [[PubMed](#)]
65. Barton, N.; Horbal, L.; Starck, S.; Kohlstedt, M.; Luzhetskyy, A.; Wittmann, C. Enabling the valorization of guaiacol-based lignin: Integrated chemical and biochemical production of cis, cis-muconic acid using metabolically engineered *Amycolatopsis* sp ATCC 39116. *Metab. Eng.* **2018**, *45*, 200–210. [[CrossRef](#)] [[PubMed](#)]
66. Prasad, S.; Roy, I. Converting Enzymes into Tools of Industrial Importance. *Recent Pat. Biotechnol.* **2018**, *12*, 33–56. [[CrossRef](#)] [[PubMed](#)]
67. Brown, J.A.; Li, D.; Alic, M.; Gold, M.H. Heat Shock Induction of Manganese Peroxidase Gene Transcription in *Phanerochaete chrysosporium*. *Appl. Environ. Microbiol.* **1993**, *59*, 4295–4299. [[CrossRef](#)]
68. Dartois, V.; Baulard, A.; Schanck, K.; Colson, C. Cloning, nucleotide sequence and expression in *Escherichia coli* of a lipase gene from *Bacillus subtilis* 168. *Biochim. Biophys. Acta* **1992**, *1131*, 253–260. [[CrossRef](#)]
69. Reddy, G.V.; Gelpke, M.D.; Gold, M.H. Degradation of 2,4,6-trichlorophenol by *Phanerochaete chrysosporium*: Involvement of reductive dechlorination. *J. Bacteriol.* **1998**, *180*, 5159–5164. [[CrossRef](#)] [[PubMed](#)]
70. Tsukihara, T.; Honda, Y.; Sakai, R.; Watanabe, T.; Watanabe, T. Exclusive overproduction of recombinant versatile peroxidase MnP2 by genetically modified white rot fungus, *Pleurotus ostreatus*. *J. Biotechnol.* **2006**, *126*, 431–439. [[CrossRef](#)]

71. Zelena, K.; Eisele, N.; Berger, R.G. *Escherichia coli* as a production host for novel enzymes from basidiomycota. *Biotechnol. Adv.* **2014**, *32*, 1382–1395. [[CrossRef](#)]
72. Wang, L.; Chang, A.K.; Yuan, W.; Bai, F. Recombinant expression, purification and characterization of a novel DyP-type peroxidase in *Escherichia coli*. *Chin. J. Biotechnol.* **2013**, *29*, 772–784.
73. Pontrelli, S.; Chiu, T.Y.; Lan, E.I.; Chen, F.Y.; Chang, P.; Liao, J.C. *Escherichia coli* as a host for metabolic engineering. *Metab. Eng.* **2018**, *50*, 16–46. [[CrossRef](#)] [[PubMed](#)]
74. Linde, D.; Pogni, R.; Cañellas, M.; Lucas, F.; Guallar, V.; Baratto, M.C.; Sinicropi, A.; Sáez-Jiménez, V.; Coscolín, C.; Romero, A.; et al. Catalytic surface radical in dye-decolorizing peroxidase: A computational, spectroscopic and site-directed mutagenesis study. *Biochem. J.* **2015**, *466*, 253–262. [[CrossRef](#)]
75. Sugano, Y.; Ishii, Y.; Shoda, M. Role of H164 in a unique dye-decolorizing heme peroxidase DyP. *Biochem. Biophys. Res. Commun.* **2004**, *322*, 126–132. [[CrossRef](#)] [[PubMed](#)]
76. Behrens, C.J.; Zelena, K.; Berger, R.G. Comparative Cold Shock Expression and Characterization of Fungal Dye-Decolorizing Peroxidases. *Appl. Biochem. Biotechnol.* **2016**, *179*, 1404–1417. [[CrossRef](#)]
77. Lin, Y.W. Rational design of heme enzymes for biodegradation of pollutants toward a green future. *Biotechnol. Appl. Biochem.* **2020**, *67*, 484–494. [[CrossRef](#)]
78. Lin, Y.W.; Nie, C.M.; Liao, L.F. Rational design of a nitrite reductase based on myoglobin: A molecular modeling and dynamics simulation study. *J. Mol. Modeling* **2012**, *18*, 4409–4415. [[CrossRef](#)]
79. Yan, D.J.; Yuan, H.; Li, W.; Xiang, Y.; He, B.; Nie, C.M.; Wen, G.B.; Lin, Y.W.; Tan, X. How a novel tyrosine-heme crosslink fine-tunes the structure and functions of heme proteins: A direct comparative study of L29H/F43Y myoglobin. *Dalton Trans.* **2015**, *44*, 18815–18822. [[CrossRef](#)] [[PubMed](#)]
80. Li, L.L.; Yuan, H.; Liao, F.; He, B.; Gao, S.Q.; Wen, G.B.; Tan, X.; Lin, Y.W. Rational design of artificial dye-decolorizing peroxidases using myoglobin by engineering Tyr/Trp in the heme center. *Dalton Trans.* **2017**, *46*, 11230–11238. [[CrossRef](#)] [[PubMed](#)]